

M. Hacımiroğlu¹, K. Artun², A.Ç. Tahaoglu³, E. Uğurlu⁴ ve C. Alban⁵

¹Phd(c) Structural + Earthquake Engineer, Designer, Ghafari Associates LLC, İstanbul*

²Msc.(SE) Structural Engineer, Designer, Ghafari Associates LLC, İstanbul

³Phd(c) Structural Engineer, Designer, Ghafari Associates LLC, İstanbul**

⁴PMP®, LEED AP BD/C, Project Manager, Ghafari Associates LLC, İstanbul

⁵Prof. Dr. Civil Engineering Dep., Consultant, İstanbul Üniversitesi – Cerrahpaşa, İstanbul

E-mail: cenkalan@iuc.edu.tr

ABSTRACT

The post-earthquake resilience of critical industrial facilities is of paramount importance. To ensure these facilities remain operational after a seismic event, innovative strategies like seismic isolation are crucial. By mitigating the damaging effects of earthquakes, seismic isolation can help achieve "immediate occupancy" performance levels, safeguarding both structural and non-structural components. This study focuses on the design of twelve large steel silos (28.5m high, 12m diameter) situated on a shared basemat in Düzce, Türkiye. The construction started in 2021 and was completed in 2023. The design process is complicated by several factors:

- Challenging Soil Conditions:** The need for pile foundations due to inadequate soil bearing capacity adds complexity to the design, requiring careful consideration of soil-structure interaction and potential differential settlement. In addition, high liquefaction potential of the site required a comprehensive site response analysis and soil improvement application.
- Near-Fault Effects:** The site's proximity to an active fault capable of generating major earthquakes introduces the possibility of near-fault effects, such as high-velocity ground motions and directivity pulses, which can significantly amplify seismic demands.
- Interdependent Silos on a Common Basemat:** The configuration of multiple silos on a single basemat necessitates a thorough analysis of the differential behavior of each silo under seismic loading to ensure overall system stability. Moreover, a full 3D model incorporating the interaction of the silos above the basemat had to be considered.
- Use of large viscous dampers:** For controlling unusually high isolator displacement demands due to poor soil conditions and closeness to an active fault.
- High vertical earthquake accelerations:** As part of the near-fault effects, vertical acceleration spectra exceeding 1g resulted in many isolators being exposed to tension forces simultaneously.
- NLTHA with 8 Different Loading Scenarios:** Because the structure contains 12 silos, and considering the operational use of the structure, Non-Linear Time History Analyses (NLTHA) were conducted for 8 different loading scenarios (full-empty-location dependent scenarios). Therefore, in addition to the single set of analyses typically performed for ordinary structures, 7 additional sets of analysis models were created and analyzed.

To address these challenges, a comprehensive design approach was adopted. Lead rubber bearings (LRBs) were selected as the primary seismic isolation devices. However, due to the region's high seismicity, supplemental viscous dampers were incorporated to control displacements and optimize system performance. Various loading scenarios were developed to evaluate the response of the isolated silos under different seismic conditions. Nonlinear time history analyses were conducted to determine critical design parameters, including isolator displacements, basemat accelerations, and potential uplift values. This project provides valuable insights into the design and implementation of seismic isolation systems for critical industrial facilities in high-seismic zones. The findings contribute to enhancing the resilience of such infrastructure, ensuring continued operation and minimizing disruptions in the aftermath of earthquakes. While the construction was in progress, the structure exhibited high performance in the Mw=6.1, 23 November 2022 in Türkiye, an earthquake that occurred after the isolators were placed.

KEYWORDS: Lead Rubber Bearing, Viscous Damper, Base Isolation, Silo Structure, Isolation Basemat

STRUCTURAL INFORMATION

Twelve large silos, each with a capacity of 1800 m³, were designed to withstand earthquakes using seismic base isolation and supplemental viscous dampers. This approach aims to minimize structural damage and ensure the continued functionality of these critical raw material storage units. A total of 12 silos, standing 28.5 meters tall with a diameter of 11.2 meters, are spaced 12 meters by 6 meters apart on a shared 2100 m² raft foundation. A girder slab flooring system distributes loads efficiently across the isolators. To validate the design's effectiveness, three-dimensional structural models were created and analyzed using nonlinear time history analysis.

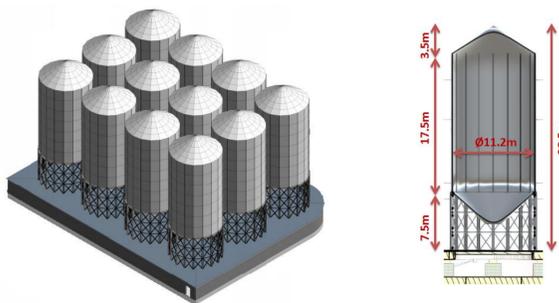


Figure 1. Three-dimensional view of the silo structure and silo dimensions

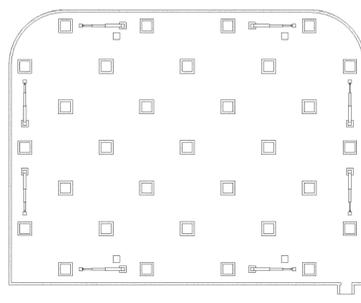


Figure 2. Base isolator and damper layout

SEISMICITY

A site-specific response spectrum was developed based on a probabilistic seismic hazard analysis conducted by Polat and Mert (2020). This spectrum was then compared to the spectrum defined in the Turkish Building Earthquake Code (TBDY 2018). The site's soil condition, classified as ZD according to the geotechnical report (Koç, 2021a), was explicitly considered in the analysis. The report also indicated the presence of liquefaction potential. A soil response analysis was performed, utilizing a Vs30 velocity of 630 m/s, consistent with the depths specified for the analysis. Eleven three-component earthquake records were selected for nonlinear time history analysis. These records were scaled to ensure they exceeded 1.3 times the TBDY 2018 spectrum. Scaling was performed within a period range of 0.5T_M to 1.25T_M for horizontal components and 0.25T_v to 1.5T_v for vertical components. Figures 2 and 3 present a comparison of the acceleration spectra obtained in the vertical and fault-perpendicular directions at Design Basis Earthquake (DBE) and Maximum Credible Earthquake (MCE) levels, respectively, with the corresponding TBDY 2018 spectra.

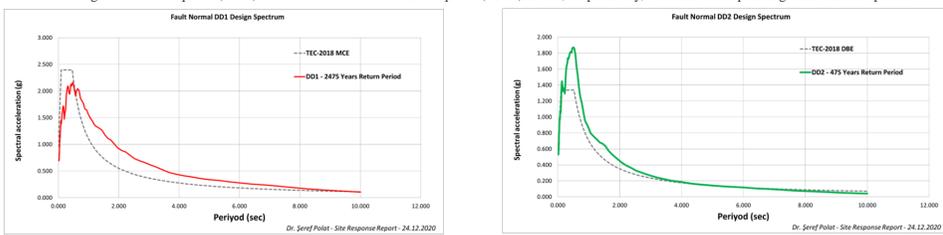


Figure 3. Comparison of the average acceleration spectra of 11 ground motion perpendicular to the fault with the TBDY2018 D type ground acceleration spectrum for DD1 and DD2 earthquake ground motion levels (Polat and Mert, 2020)

STRUCTURAL DESIGN

To determine the effective stiffness of concrete elements, Table 13.1 from Article 14.3.9 of the Turkish Building Earthquake Code (TBDY2018) was utilized. The code's specified load combinations for structural design above and below the isolation plane were also incorporated. A detailed three-dimensional (3D) model of the base-isolated silo was developed and analyzed using the SAP2000 finite element software (CSI, 2021). Earthquake forces governing the design of the superstructure were determined by analyzing the base shear transferred through the isolation system during time history analysis. The selected foundation thickness is 100-150 cm, beam dimensions are 200x100 cm and slab thickness is 35 cm. In addition to TBDY2018, the design process also referenced several other relevant standards, including ASCE 7-10 (2010), ACI318-08 (2008), ASD89 (1989), Eurocode 8 (2003), TS500 (2000), and TS498 (1997).

STRUCTURE - PILE - SOIL INTERACTION CALCULATIONS

The design of the silo structure presented a unique challenge due to the combination of variable loading conditions and the presence of seismic isolators. To effectively manage potential differential settlements and ensure foundation stability, a comprehensive approach was adopted, which included soil improvement measures and the incorporation of pile foundations. This necessitated a detailed analysis of the structure-pile-soil interaction. The analysis was conducted, employing an iterative approach (Koç, 2021b) based on "Structure-Pile-Soil Interaction - Method III" outlined in TBDY2018. This method involves a joint system model that considers the pavement, foundation, piles, and soil, represented by linear springs (p-y, t-z, and Q-Z) to capture the inertial interaction effects. In accordance with Article 16C.4.3.1 of TBDY2018, the initial stiffness of these springs was used to model the linear behavior of the piles. A total of 124 piles, each with a length of 32 meters, were incorporated into the design. The analysis also accounted for the group effect, considering the specific arrangement and spacing of the piles. This comprehensive approach ensured that the foundation system could effectively handle the complex loading conditions and maintain stability, even under seismic events.

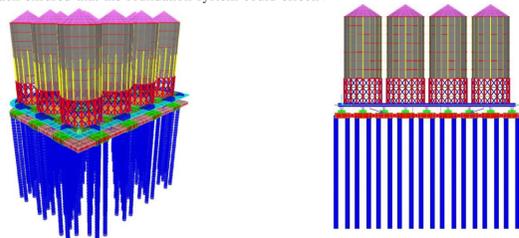


Figure 4. Equivalent linear pile spring values (Koç, 2021) and structural analysis model (3D and Section)

To determine the forces acting on the piles due to seismic inertia effects, a response spectrum analysis was performed. The analysis model considered the mass of the foundation but neglected the mass of the piles themselves. Earthquake data was incorporated using the spectrum defined in Article 16C.4.2.3 of TBDY2018. This design spectrum was derived by averaging the surface-recorded ground motions obtained from the soil behavior analysis. The inertial interaction analysis yielded internal forces within the piles for each earthquake direction. These forces were then combined with the internal forces obtained from a separate kinematic analysis, as per Article 16C.5 of TBDY2018. This combination of inertial and kinematic effects provided a comprehensive understanding of the loads acting on the piles, ultimately informing the final pile design.

BASE ISOLATION

The design of the base-isolated silo structure aimed to achieve the "immediate occupancy" (IK) performance level as defined in Section 3.4 of TBDY2018. This performance level requires considering the DD2 earthquake (Maximum Credible Earthquake - MCE) for the superstructure (silos) and the DD1 earthquake (Design Basis Earthquake - DBE) for the isolation system and substructure (isolators, pedestals, and foundation). The design process focused on meeting performance targets, such as maximum base shear force ratios, while considering the regional seismic hazard and soil conditions. Selection of the isolation period and effective damping ratio targets was guided by typical product characteristics offered by isolator suppliers. The theoretical basis for the base isolation design is detailed in the study by Naem and Kelly (1999). To evaluate the performance of the isolation system under various loading conditions, time history analyses were conducted, considering both full and empty silo scenarios. Eight different loading conditions, as illustrated in Figure 5, were analyzed to assess isolator displacement capacity, acceleration levels transmitted to the superstructure, and base shear forces. This comprehensive analysis ensured that the design objectives were met under a range of operational and seismic conditions. 11 DD1 and 11 DD2 three-direction register sets were introduced to the structural analysis model using the necessary scale factors and analyses were performed. In addition, in accordance with TBDY 2018 Article 5.7.2.1, the records in the horizontal direction were rotated 90° and the analyses were repeated.

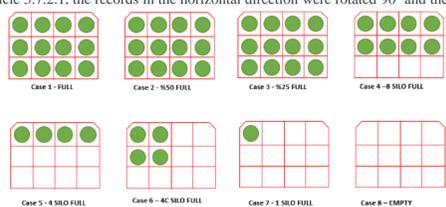


Figure 5. Silo loading states

BASE ISOLATION AND VISCOUS DAMPER PROPERTIES

The isolation system of the silo structure utilizes Lead Rubber Bearing (LRB) isolators. LRBs were chosen due to their ability to better handle tensile forces that occur in many isolators simultaneously, especially in regions with high vertical earthquake movements. Friction pendulum isolators were initially considered but not selected due to the widespread occurrence of uplift in the isolators. A total of 31 LRB isolators are used in the system, categorized into two types based on their axial load capacity under seismic conditions:

- Type 1: Designed for axial loads ranging from 13500 kN to 18000 kN.
- Type 2: Designed for axial loads ranging from 3000 kN to 13500 kN.

To optimize isolator displacements in the high-seismicity region, 16 viscous dampers were added at the isolation level.

The selected LRB isolators were rigorously evaluated to ensure their suitability for the project. Table 2 provides a summary of the key isolator parameters and their corresponding dynamic values. To determine the maximum displacement, calculations were performed using the Lower Bound (LB) properties of the isolators and the DD1 maximum direction spectrum. Conversely, the maximum base shear force was calculated using the Upper Bound (UB) properties and the DD2 maximum direction spectrum. In line with the earthquake code (TBDY2018), the unit strain limits of the elastomer isolation units were checked. The resulting unit strain value ($\gamma_{s,p}$) due to horizontal displacement under seismic loading remained below the allowable limit of 2.0, confirming the isolators' ability to withstand the anticipated deformations.

Parameter	Value
Number of Isolators	31
Boundary Range (UB / LB)	15 / 0.8
Rubber Shear Modulus (G _r)	0.45 Mpa
Total Rubber Height (T _r)	500 mm
Isolator Displacement Capacity (D)	90 cm
Lead Shear Yield Stress (T _{yp})	10 Mpa
Seismic Device Brand Name	DIS (Dynamic Isolation Systems)

To mitigate isolator displacement at the Design Basis Earthquake (DBE) level and enhance the structural response under the Maximum Credible Earthquake (MCE), supplemental viscous dampers were incorporated at the isolation level. Nonlinear time history analyses were conducted to optimize the damping characteristics and determine the appropriate number of dampers. Table 3 presents the design parameters of these viscous dampers, which work in conjunction with the Lead Rubber Bearing (LRB) isolators to achieve the desired performance objectives.

Parameter	Value
Boundary Range (UB / LB)	110 / 0.85
Damper Displacement Capacity	± 100 cm
Damper Speed, V	1.40 m/s
Velocity Exponent, α	0.3
Force Acting on a Single Damper	4400 kN
Seismic Device Brand Name	Maurer

Dampers are placed at an angle of 17° vertically and at an angle of 45° in plan (Figure 6). The total system damping rate from the isolators and a total of 8 dampers were taken as 30% and the maximum total displacement (D_{Tot}) was calculated as 96 cm using the effective equivalent earthquake load method.

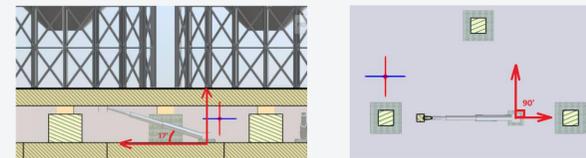


Figure 6. Placement of dampers in cross-section and plan

RESULTS

Isolator Maximum Displacements

To assess the potential torsional effects on the structure, maximum isolator displacements were monitored at the corner points (Figures 7, 8, and 9). These maximum displacements were determined by calculating the resultant of the displacements in the x and y directions at each time step. Nonlinear time history analyses revealed a maximum isolator displacement of 83.5 cm.

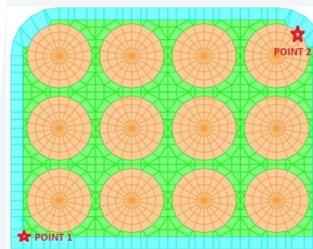


Figure 7. Monitored Slab Points

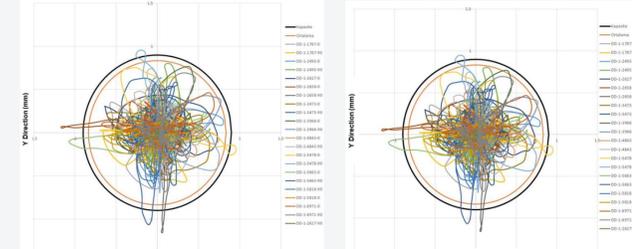


Figure 8. "Point 1" and "Point 2" isolator resultant displacement (LRB)

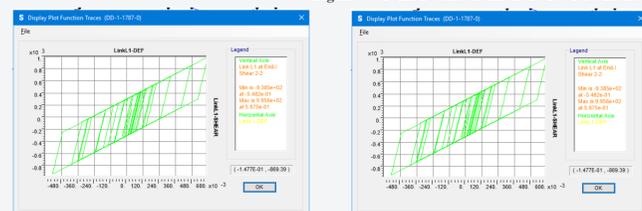


Figure 9. Force - Displacement graph of an example isolator and damper (DD1-LB)

Maximum Floor Acceleration

To evaluate the maximum acceleration experienced at each level of the structure, a resultant acceleration was calculated for each earthquake record by combining the x and y direction accelerations. The maximum acceleration at the silo level was then determined by averaging the resultant accelerations across all 11 earthquake records. Table 4 presents the acceleration values for different loading conditions (refer to Figure 5) at both the below-isolator level (Z1) and the above-isolator level (Z2). Since the silo design is governed by the accelerations experienced at the base of the silos, the values corresponding to the DD2 earthquake and the upper bound properties of the isolators are presented. The acceleration values are expressed as a fraction of gravitational acceleration ($g = 9.81 \text{ m/s}^2$). The table clearly demonstrates the effectiveness of the isolation system in reducing the transmission of ground accelerations to the superstructure, even under the most critical loading scenarios. To validate the effectiveness of the seismic isolation system during the design phase, a comparative analysis was conducted. A model of the silo complex without seismic isolation was developed, and the acceleration distributions in both models were examined under identical earthquake records. This analysis revealed a significant reduction in acceleration values throughout the seismically isolated silo complex, with accelerations being reduced by approximately half. The benefit of seismic isolation was particularly evident at the top of the silos, where the reduction in acceleration was even greater. This targeted reduction in acceleration at the top of the silos aims to ensure the uninterrupted operation of critical equipment, such as conveyor systems, even after a seismic event.

Table 4 - Calculated acceleration values in non-linear time history

Point	Level	Case 1	Case 2	Case 3	Case 4	Case 5	Case 6	Case 7	Case 8
#	m	g	g	g	g	g	g	g	g
ZZ	0	0.466	0.507	0.505	0.515	0.618	0.585	0.616	0.465
Z1	-3	0.641	0.641	0.641	0.641	0.641	0.641	0.641	0.641

Construction and Experience of Mw=6.1, 23 November 2022 Earthquake

As seen in Figure 10, the silo construction has been completed and materials have begun to be stored in the silos. The total construction time, including soil improvement, took approximately two years. After the LRB (Lead Rubber Bearing) type isolators were installed, the basemat construction and silo installation were finalized. However, the production and testing of the viscous dampers were completed later, and their installation took place after the construction of the silos was finished. For this installation work, a floor opening was planned to allow easy mobilization of the dampers. The design of the silos was based on the forces obtained from Time History Analysis. In particular, the basemat design and rebar placement were carried out in accordance with the base plate layout of the silos. Adequate clearances were provided to accommodate the top displacement values of the silos. Necessary silo equipment was detailed considering seismic movement to ensure the functional operation of the silo system. During the Mw=6.1 Düzce earthquake that occurred on November 23, 2022, the structure, which was still under construction, exhibited performance at the Immediate Occupancy level. A site investigation confirmed that no damage, not even hairline cracks, occurred.



Figure 10. Site and Isolator Floor Photo

ACKNOWLEDGMENTS

We would like to thank Civil Engineer Enrico Dalmasso and Civil Engineer Swapnil Gaur, one of the executives of Ferrero Fındık İthalat İhracat ve Ticaret AŞ, for their valuable contributions during the study phase.

REFERENCES

- ASCE 7-10 (2010), "Minimum design loads for buildings and other structures," American Society of Civil Engineers, ASCE Standard No. ASCE/SEI 7-10, Reston, VA.
- ACI318-08 (2008), "Building Code Requirements for Structural Concrete and Commentary," American Concrete Institute.
- CSI (2021), "SAP2000 23.0.0: Integrated Software for Structural Analysis and Design," Computers and Structures Inc., Berkeley, CA.
- TBDY (2018), "Deprem Etkisi Altında Binaların Tasarımı İçin Esaslar," T.C. Bayındırlık ve İskan Bakanlığı.
- Eurocode 8 (2003), "Design of Structures For Earthquake Resistance Part 1: General Rules, Seismic Actions And Rules For Buildings".
- TS500 (2000), "Betonarme Yapıların Tasarım ve Yapım Kuralları," Türk Standartları Enstitüsü.
- TS498 (1997), "Yapı Elemanlarının Boyutlandırılmasında Alınacak Yüklerin Hesap Değerleri," Türk Standartları Enstitüsü.
- Naem, F. and Kelly, J.M. (1999), Design of Seismic Isolated Structures: From Theory to Practice, John Wiley and Sons, Inc., New York.
- Polat Ş., Mert A. (2020) Üretim Tesisi Deprem Tehlike Değerlendirmesi ve Zemin Bağımlı Tasarım Yer Hareketlerinin Belirlenmesi, Boğaziçi Üniversitesi Deprem Mühendisliği Anabilim Dalı
- Koç M., Karsavuran B., Budak M., Üner D. (2021a) Desteç Consulting Engineering and Project INC., Geotechnical Interpretation Report
- Koç M., Çelik B. (2021b) Desteç Consulting Engineering and Project INC., Soil Structure Interaction Report